

# Single-cell RNA-seq of the Developing Cardiac Outflow Tract Reveals Convergent Development of the Vascular Smooth Muscle Cells at the Base of the Great Arteries

Xuanyu Liu<sup>1</sup>, Wen Chen<sup>1</sup>, Wenke Li<sup>1</sup>, James R. Priest<sup>2</sup>, Jikui Wang<sup>3</sup>, Zhou Zhou<sup>1</sup>

1. State Key Laboratory of Cardiovascular Disease, Beijing Key Laboratory for Molecular Diagnostics of Cardiovascular Diseases, Center of Laboratory Medicine, Fuwai Hospital, National Center for Cardiovascular Diseases, Chinese Academy of Medical Sciences and Peking Union Medical College, Beijing 100037, China
2. Stanford University School of Medicine, Stanford, CA 94305, USA
3. Henan Key Laboratory for Medical Tissue Regeneration, School of Basic Medical Sciences, Xinxiang Medical University. Xinxiang 453003, China

**Running title:** Single-cell RNA-seq of the developing cardiac outflow tract

## Subject Terms:

Developmental Biology, Vascular Biology, Gene Expression and Regulation, Congenital Heart Disease

## Address correspondence to:

Dr. Jikui Wang  
School of Basic Medical Sciences  
Xinxiang Medical University  
No. 601, Jinsui Road  
453003 Xinxiang  
China  
Tel: +86 18336067869  
Fax: +86 010-88398055  
wangjikui00@gmail.com

Dr. Zhou Zhou  
Fuwai Hospital  
Chinese Academy of Medical Sciences  
No. 167 Beilishi Street, Xicheng District  
100037 Beijing  
China  
Tel: +86 010-88398055  
Fax: +86 010-88398055  
zhouzhou@fuwaihospital.org

## 1 ABSTRACT

2 **Rationale:** Cardiac outflow tract (OFT) is a major hotspot for congenital heart diseases (CHDs).  
3 A thorough understanding of the cellular diversity, transitions and regulatory networks of  
4 normal OFT development is essential to decipher the etiology of OFT malformations.

5 **Objective:** We sought to explore the cellular diversity and transitions between cell lineages  
6 during OFT development.

7 **Methods and Results:** We performed single-cell transcriptomic sequencing of 55,611 mouse  
8 OFT cells from three developmental stages that generally correspond to the early, middle and  
9 late stages of OFT remodeling and septation. We identified 17 cell clusters that could be  
10 assigned to six cell lineages. Among these lineages, the macrophage and VSMC lineages of the  
11 developing OFT have seldom been previously described. Known cellular transitions, such as  
12 endothelial to mesenchymal transition, have been recapitulated. In particular, we identified  
13 convergent development of the VSMC lineage, where intermediate cell subpopulations were  
14 found to be involved in either myocardial to VSMC trans-differentiation or mesenchymal to  
15 VSMC transition. Through single-molecule *in situ* hybridization, we observed that cells  
16 expressing the myocardial marker *Myh7* co-expressed the VSMC marker gene *Cxcl12* in OFT  
17 walls, thus confirming the existence of myocardial to VSMC trans-differentiation. Moreover,  
18 we found that the *Penk<sup>+</sup>* cluster c8, a relatively small mesenchymal subpopulation that was  
19 undergoing mesenchymal to VSMC transition, was associated with the fusion of OFT cushions.  
20 We also uncovered the expression dynamics and critical transcriptional regulators potentially  
21 governing cell state transitions. Finally, we developed web-based interactive interfaces to  
22 facilitate further data exploration.

23 **Conclusions:** We provide a single-cell reference map of cell states for normal OFT  
24 development, which will be a valuable resource for the CHD community. Our data support the  
25 existence of myocardial to VSMC trans-differentiation and convergent development of the  
26 VSMC lineage at the base of the great arteries.

27 **Keywords:**

28 cardiac outflow tract; single-cell RNA-seq; trans-differentiation; vascular smooth muscle;  
29 convergent development

30 **Nonstandard Abbreviations and Acronyms:**

31	EndoMT	endothelial to mesenchymal transition
32	GRN	gene regulatory network
33	KNN	k nearest neighbor
34	OFT	outflow tract
35	SHF	second heart field
36	UMI	unique molecular identifier
37	VSMC	vascular smooth muscle cell

## 38 INTRODUCTION

39 Congenital heart disease (CHD) is the most common form of human birth defects (~1% of live  
40 births) and represents the leading cause of mortality from birth defects worldwide<sup>1</sup>.  
41 Approximately 30% of CHDs involve abnormalities in cardiac outflow tract (OFT)  
42 development, thus constituting a large class of CHDs, namely OFT malformations, such as  
43 persistent truncus arteriosus (PTA), double outlet right ventricle (DORV), transposition of the  
44 great arteries (TGA) and aortopulmonary-window (APW)<sup>2,3</sup>. It is therefore acknowledged that  
45 OFT is a major hotspot for human CHDs<sup>4</sup>. OFT malformations require surgical repair once  
46 diagnosed and usually have a poor prognosis<sup>5</sup>. However, the etiology for the majority of this  
47 severe class of CHDs remains unknown.

48 Cardiac OFT is a transient conduit during embryogenesis at the arterial pole of the heart,  
49 connecting the aortic sac with embryonic ventricles, which undergoes rotation and septation  
50 (a.k.a., OFT remodeling) to give rise to the base of the pulmonary trunk and ascending aorta;  
51 thus, this process is critical for the establishment of separate systemic and pulmonary  
52 circulations<sup>6</sup>. The high incidence of OFT malformations may be explained by the complexity  
53 of OFT development, which requires intricate interplay and transitions among diverse cell  
54 populations, including cardiac cells and migrating extra-cardiac cells, making it particularly  
55 susceptible to genetic or environmental perturbations. A thorough understanding of the cellular  
56 diversity, cellular transitions and regulatory networks of normal OFT development is essential  
57 to decipher the etiology of OFT malformations.

58 Multiple disparate cell types have been implicated in OFT development through tightly  
59 coordinated processes such as migration, differentiation and transition. Initially, the OFT wall  
60 basically consists of a solitary tube of myocardium derived from the second heart field (SHF)<sup>7</sup>.  
61 At the initiation of remodeling, the interstitial space between the myocardium and endothelium  
62 is filled with extracellular matrix (“cardiac jelly”) secreted by mesenchymal cells that form  
63 OFT cushions at the proximal and distal regions<sup>8</sup>. Cardiac neural crest cells (CNCCs) migrate  
64 into the cardiac OFT, where they first join the mesenchyme of the distal and then the proximal  
65 cushions, playing an essential role in the fusion of the distal cushions to form a smooth muscle  
66 septum, i.e., aorticopulmonary septum, which divides the aorta and pulmonary trunk<sup>9,10</sup>. In  
67 addition to CNCCs, distal OFT cushions are colonized by cells derived from the SHF, which  
68 eventually give rise to smooth muscle walls of the base of the great arteries<sup>11</sup>. In contrast,  
69 proximal OFT cushions are mainly populated by the mesenchymal progenies of OFT  
70 endothelial cells that undergo endothelial to mesenchymal transition (EndoMT)<sup>12</sup>. Besides, the  
71 OFT remodeling is accompanied by other biological processes, for example, the maturation of  
72 the smooth muscle walls, since the OFT wall changes from a myocardial to an arterial  
73 phenotype with development<sup>13</sup>. Given the complexity of OFT development, we expect a  
74 heterogeneous cellular composition represented by multiple subpopulations of the same cell  
75 type and extensive cellular transitions occurring between different cell types. However, the cell  
76 type and cell states of the cardiac OFT during development have not yet been systematically  
77 dissected.

78 Recent technical advances have enabled the transcriptomes of tens of thousands of cells to be  
79 assayed at single-cell resolution in a single experiment<sup>14</sup>. Single-cell RNA-seq has shown itself  
80 to be a powerful tool to provide insights into the processes underlying developmental,  
81 physiological and disease systems<sup>15</sup>. Single-cell RNA-seq enables the dissection of cellular  
82 heterogeneity in an unbiased manner with no need for any prior knowledge of the cell  
83 population<sup>16</sup>. Unsupervised clustering of cells based on genome-wide expression profiles  
84 enables the identification of novel cell types or subpopulations, as well as gene signatures for  
85 all cell types. Beyond cellular heterogeneity dissection, single-cell RNA-seq data empower  
86 systematic interrogations of the developmental trajectory of cell lineages in tissue systems and  
87 the regulatory networks underlying the cell state transition processes<sup>17</sup>. Although traditional  
88 gene knockdown studies have uncovered regulators during OFT development<sup>10</sup>, how genes are  
89 regulated under a normal developmental context remains unclear. Single-cell RNA-seq has  
90 been applied to study the cellular diversity of embryonic<sup>18, 19</sup> or adult heart<sup>20, 21</sup> at the whole  
91 organ level; however, few or a limited number of cardiac OFT cells have been sampled in these  
92 studies.

93 Here, we performed single-cell transcriptomic sequencing of 55,611 mouse OFT cells from  
94 three successive developmental stages corresponding to the early, middle and late stages of OFT  
95 remodeling and septation. We sought to unbiasedly and systematically dissect the cell types and  
96 states during OFT development. We explored the cell lineage relationships and cellular state  
97 transitions during OFT development, as well as the critical transcription regulators underlying  
98 the transitions. We identified convergent development of the vascular smooth muscle cells  
99 (VSMCs) at the base of the great arteries, where intermediate cell subpopulations were found  
100 to be involved in either myocardial to VSMC trans-differentiation or mesenchymal to VSMC  
101 transition. Our study provided a single-cell reference map of cell transcriptomic states for OFT  
102 normal development.

## 103 METHODS

104 See **Online Methods**.

105 The sequencing read data have been deposited in Genome Sequence Archive (GSA;  
106 <http://gsa.big.ac.cn/>) and are accessible through accession number CRA001120.

## 107 RESULTS

108 ***Single-cell transcriptomic sequencing and unbiased clustering of developing OFT***  
109 ***cells.***

110 To obtain a map of the cellulome for the developing OFT during remodeling and septation, we  
111 isolated and sequenced a total of 64,605 cells from three successive developmental stages,

112 namely, ps47 (47 pairs of somites), ps49 and ps51, which generally correspond to the early  
113 (initiation), middle and late (almost completion) stages of septation, respectively (Figure 1A).  
114 Sequencing quality metrics were similar across samples, reflecting little technical variation  
115 among samples (Online Table I). After stringent quality filtering and discarding a small number  
116 (297) of red blood cells, we obtained a high-quality transcriptomic dataset for 55,611 cells.

117 Based on the single-cell transcriptional profiles, unsupervised clustering identified 17 cell  
118 clusters at the chosen resolution (Figure 1B) that represent distinct cell types or cell  
119 subpopulations. Next, we compared the relative proportions of cells from different samples in  
120 each cluster (Figure 1C). Importantly, there was no significant difference in cell fraction  
121 between the two biological replicates for each stage, reflecting the validity of cell clustering  
122 (Wilcoxon signed rank test P-value = 0.25). Moreover, all the clusters contained cells from the  
123 three stages except c14, a small cluster (342 cells), suggesting that the samples for each stage  
124 covered all common cell states throughout development. However, the relative proportions  
125 varied greatly between stages, as reflected by the observation that the cell fractions for some  
126 clusters, e.g., c11, remarkably changed during development (Figure 1C).

127 ***Cellular diversity and heterogeneity during OFT development identified by single-***  
128 ***cell transcriptomic analysis.***

129 To define the identity of each cell cluster, we performed differential expression analysis  
130 between each cluster and all others (Online Table II), and assigned a specific cell type to each  
131 cluster based on the established lineage-specific marker genes (Figure 2A). Cluster c15  
132 represented a small group of macrophages that resided in the developing OFT as the cells in  
133 this cluster specifically expressed *Fcgr1* and *Adgre*<sup>21, 22</sup>. Clusters c10 and c11 constituted the  
134 epicardial lineage as they specifically expressed *Upk3b* and *Upk1b*<sup>19, 23</sup>. Clusters c5, c6 and c12  
135 highly expressed *Ecsr* and *Cdh5*<sup>19, 24</sup>; thus, they belonged to the endocardial lineage. Clusters  
136 c2, c9, c14 and c16 highly expressed myocardial marker genes, such as *Myh7* and *Myl4*<sup>19, 25</sup>.  
137 The mesenchymal lineage comprised four closely aligned clusters, namely, c0, c1, c7 and c8,  
138 which highly expressed mesenchymal marker genes, such as *Postn* and *Cthrc1*<sup>19</sup>. The VSMC  
139 lineage included c3, c4 and c13, which specifically expressed *Rgs5*, a gene that is abundantly  
140 expressed in arterial smooth muscle cells<sup>26, 27</sup>, and *Cxcl12*, a chemokine encoding gene that is  
141 highly expressed in the walls of the aorta and pulmonary trunk of the embryonic heart (E12.5)<sup>28</sup>.  
142 We also assessed the expression intensity distribution of contractile markers for smooth muscle  
143 cells, including *Acta2*, *Tagln*, *Cnn1* and *Myl9*<sup>25, 29</sup>. We observed the expression of these markers  
144 in our VSMC lineage clusters. However, the specificity of these markers was not ideal since  
145 they were also highly expressed in myocardial and mesenchymal lineages (Online Figure IA),  
146 which is in line with previous knowledge<sup>29</sup>. Moreover, only a small group of cells expressed  
147 *Myh11*, the most specific contractile marker for mature VSMCs<sup>29</sup>, and clustered on the edge of  
148 c3, which may represent a group of relatively mature VSMCs. By contrast, the expression of  
149 contractile markers for embryonic myocardial cells<sup>25</sup>, including *Myh7*, *Tnncl*, *Tnnt2*, *Myl2* and

150 *Myl4*, were relatively specific in myocardial lineage clusters (Online Figure IB). Ultimately, we  
151 identified clusters of VSMCs at the base of the great arteries, most of which may exhibit an  
152 immature, synthetic phenotype at this developmental stage.

153 The six cell lineages identified by established marker genes were further confirmed by  
154 hierarchical clustering analysis, which showed that the clusters assigned to the same lineage  
155 were grouped together and closely aligned on the tree (Figure 2B). Once cell identity was  
156 assigned, we explored the relative proportions of each cell lineage during development (Figure  
157 2B & 2C). The mesenchymal lineage in OFT cushions constituted the most abundant cell type  
158 (46.3%), and the relative proportion significantly decreased at the late stage (Student's t-Test P-  
159 value < 0.05), suggesting that an active cellular transition occurred at the late stage. The  
160 macrophages accounted for only 0.5% of all cells, and the relative proportion did not  
161 significantly change during development. Strikingly, the myocardial lineage diminished over  
162 time, while the VSMC lineage expanded during development, in accordance with the  
163 myocardial to arterial phenotypic change. The epicardial lineage also significantly expanded  
164 with development, consistent with a previous report<sup>19</sup>.

165 ***Machine learning-based selection of molecular signatures for cell lineages and***  
166 ***clusters during OFT development.***

167 To select molecular signatures that define the identified cell lineages and clusters, we adopted  
168 a machine learning-based strategy (Online Figure II). All the random forest models we trained  
169 achieved a good classification performance (AUC range: 0.94–1; Online Figure III & Online  
170 Figure IV). The top genes that contributed the most to the models were selected as the molecular  
171 signatures for each of the six cell lineages or each subpopulation/cluster (Figure 2D). For cell  
172 lineages, most selected genes have been reported to be specifically expressed in a cell type. For  
173 example, *Wt1* in epicardium<sup>30</sup>, *Vcan* in cushion mesenchyme<sup>31</sup>, *Myh7* in myocardium<sup>32</sup>, *Rasip1*  
174 in endocardium<sup>33</sup> and *Fbln5* in VSMCs<sup>34</sup>. However, some genes have seldom been previously  
175 described to be expressed specifically in a cell lineage of the developing OFT, e.g., *Aldh1a2* in  
176 epicardium and *Papss2* in mesenchyme. For clusters of each lineage, some selected markers  
177 have been reported to be cell type-specific in the embryonic heart (E10.5)<sup>19</sup>; however, they were  
178 found to be expressed in a cluster-specific manner. For example, *Tmem255a* was reported to be  
179 the epicardium marker of the E10.5 heart<sup>19</sup>; however, in the present study, it was specifically  
180 expressed in only one of the two subpopulations of the epicardial cells, namely, c10 (Online  
181 Figure IV).

182 ***Convergent development of the VSMCs at the base of the great arteries inferred from***  
183 ***a KNN graph.***

184 To infer the relationships of cell lineages, we visualized the single-cell dataset using a force-

185 directed layout of a k-nearest-neighbor (KNN) graph (Figure 3A & 3B), which has been proven  
186 to perform better than t-distributed stochastic neighbor embedding (tSNE) for visualizing  
187 complex and continuous gene expression topologies of cell populations<sup>35</sup>. Cell clusters of the  
188 same lineage were closely aligned in the KNN graph, and known relationships among lineages  
189 have been well recapitulated. For example, the EndoMT process was reflected by an abundance  
190 of potentially intermediate, transitioning cells connecting the endocardial lineage (c5) and  
191 mesenchymal lineage (c1), while these cell clusters were separated in the tSNE plot shown in  
192 Figure 1B. The dynamic changes in cell states during development could be well visualized  
193 when the cells were displayed by developmental stage (Figure 3C). For example, we observed  
194 the rapidly diminished myocardium and the expanded epicardium.

195 In particular, we noticed five cell clusters, including c1, c3, c4, c8 and c9, which may be directly  
196 related to the development of VSMCs (Figure 3D & 3E). VSMC cluster c4 expanded during  
197 the early and middle stage and was almost replaced by VSMC cluster c3 at the late stage. In the  
198 KNN plot (Figure 3D), c4 became closer to c3 over time. Therefore, we speculated that c4 may  
199 represent an intermediate state and c3 a more mature state of VSMCs. Intriguingly, myocardial  
200 subpopulation c9 and VSMC progenitor population c4 were densely connected, and a  
201 considerable number of cells were in between, which may represent intermediate, transitioning  
202 cell states. Therefore, this finding could imply that myocardial to VSMC trans-differentiation  
203 may occur during OFT development. Moreover, a relatively small (1,924 cells) mesenchymal  
204 cluster, c8, was closely aligned with c4 and became closer to c4 over time, implying that c8  
205 may represent a special mesenchymal subpopulation actively involved in the mesenchymal to  
206 VSMC transition at a relatively early stage. Additionally, c1, a relatively large (10,407 cells)  
207 mesenchymal subpopulation may also be involved in the mesenchymal to VSMC transition,  
208 particularly at a relatively late stage, as reflected by an abundance of potentially intermediate  
209 cells connecting c1 and c3, mainly at stage ps51 (Figure 3D).

210 Altogether, our data suggest convergent development of the VSMCs at the base of the great  
211 arteries, where intermediate cell subpopulations were found to be involved in either  
212 mesenchymal to VSMC transition or myocardial to VSMC trans-differentiation. The inferred  
213 development paths of VSMCs are summarized in Figure 3F. Since a considerable number of  
214 intermediate cells were captured in our dataset, these biological processes could even be  
215 directly inferred from the tSNE plot (Figure 3G).

216 ***Characteristics of gene expression profiles for intermediate cell subpopulations***  
217 ***involved in the myocardial to VSMC trans-differentiation***

218 We next sought to confirm myocardial to VSMC trans-differentiation by examining the gene  
219 expression profiles of the intermediate cell subpopulations that we identified above, c9 and c4.  
220 Cell cluster c9 and the largest myocardial cluster c2 displayed distinct expression profiles  
221 (Figure 4A). Compared with c2, c9 showed significant up-regulation of VSMC marker genes,

222 including contractile VSMC markers<sup>29</sup> (e.g., *Acta2*, *Tagln*, *Cald1* and *Myl9*) and synthetic  
223 VSMC markers<sup>36</sup> (e.g., *Eln*, *Colla2* and *Cxcl12*; Figure 4A, B). Myocardium-specific genes,  
224 *Tnncl* and *Tnnt2*<sup>25</sup>, were expressed at significantly higher levels in c9 than in c2, reflecting the  
225 myocardial identity of c9. However, some myocardial markers, such as *Myl2*, were significantly  
226 down-regulated in c9. Moreover, the ratio of *Myh6* to *Myh7*, an index reflecting the degree of  
227 maturation and functionality of cardiomyocytes<sup>37</sup>, was significantly lower in c9 (Wilcoxon rank  
228 sum test P-value < 2.2e-16; Figure 4C), suggesting that c9 cells may exhibit a less “mature”  
229 phenotype and be undergoing phenotypic changes. The genes up-regulated in c9 versus c2  
230 (Online Table III) were enriched for pathways such as smooth muscle contraction, elastic fiber  
231 formation and artery morphogenesis (Figure 4D).

232 We also observed distinct expression profiles between the two VSMC clusters, c3 and c4  
233 (Figure 4E, Online Table IV). Genes related to the development and maturation of VSMCs,  
234 such as *Fbln5*, *Eln*, *Col3a1* and *Colla1*, were significantly up-regulated in c3 versus c4 (Figure  
235 4E &4F). The genes up-regulated in c3 were mainly enriched for ECM organization (Figure  
236 4G). These results support our inference that c3 represents a more mature state of VSMCs than  
237 c4 does. Compared with c3, c4 exhibited significantly higher expression of both myocardial  
238 markers (e.g., *Tnncl* and *Tnnt2*<sup>25</sup>) and mesenchymal markers (e.g. *Cthrc1* and *Sox9*<sup>19</sup>),  
239 reflecting its myocardial and mesenchymal heritage.

240 Altogether, the expression profile analysis supports our inference that c9 and c4 cells are in an  
241 intermediate state along the trajectory of myocardium to VSMC trans-differentiation.

242 ***Pseudo-temporal ordering and gene regulatory network analysis uncover critical  
243 transcriptional regulators potentially governing cell state transitions during OFT  
244 development.***

245 To elucidate gene expression dynamics, especially the transcriptional regulators governing the  
246 convergent development of VSMCs, we reconstructed the development trajectories for the  
247 different paths (Figure 3G) through pseudo-temporal ordering of individual cells using  
248 CellRouter (See Methods). For the myocardial to VSMC trans-differentiation (c9-c4-c3), we  
249 identified genes that were significantly correlated with the trajectory (Online Table V) and  
250 observed the loss of myocardial marker expression and gain of VSMC marker expression  
251 during the progression of trans-differentiation (Figure 5A). The Notch signaling pathway  
252 positively regulates the specification, differentiation, and maturation of VSMCs<sup>38</sup>. Strikingly,  
253 we noted that the expression of genes in the Notch signaling pathway, including receptor  
254 (*Notch1*), ligand (*Jag1*) and downstream targets (*Hey1*, *Hey2*, *Heyl* and *Pdgfrb*), was positively  
255 correlated with the trajectory (Figure 5B). Furthermore, by gene regulatory network (GRN)  
256 analysis, we obtained a set of key regulators that were activated sequentially along the trajectory  
257 and potentially drove the process (Figure 5C). We identified *Heyl*, encoding a known  
258 downstream TF of Notch signaling, at the top of the up-regulated regulators, consistent with its

259 known positive role in VSMC development<sup>38</sup>. *Tbx20*, encoding a TF known as a transcriptional  
260 repressor in the developing heart<sup>39</sup>, was at the top of the down-regulated regulators, implying  
261 its role in repressing VSMC lineage-specifying genes. Regulators that were activated early in  
262 the trajectory, such as *Plagl1* and *Naca*, may play potential roles in lineage commitment.

263 For mesenchymal (the c8 *Penk*<sup>+</sup> subpopulation) to VSMC transition (c8-c4-c3), we identified  
264 genes that were significantly correlated with the trajectory (Online Table VI) and observed the  
265 loss of mesenchymal marker expression and gain of VSMC marker expression during the  
266 progression of the transition (Figure 5D). The expression of genes in the Notch signaling  
267 pathway was positively correlated with the trajectory (Figure 5E). Interestingly, we found *Heyl*  
268 and *Tbx20* also ranked at the top of the key regulators (Figure 5F). Consistent with our  
269 knowledge, the positive regulator *Mef2c*, a TF essential for VSMC development<sup>40</sup>, was  
270 activated relatively early in the reconstructed trajectory.

271 Similarly, for c1 mesenchymal to VSMC transition (c1<sub>ps51</sub>-c3), we observed the loss of  
272 mesenchymal marker expression and gain of VSMC marker expression during the progression  
273 of the transition (Online Figure VA, Online Table VII). The expression of genes in the Notch  
274 signaling pathway was positively correlated with the trajectory (Online Figure VB). By contrast,  
275 the top regulators were different from those in the c8 mesenchymal to VSMC transition (Online  
276 Figure VC).

277 Additionally, we reconstructed the trajectory and identified the gene expression dynamics for  
278 the EndoMT process between c5 endothelial cells and c1 mesenchymal cells (Online Table VIII,  
279 Online Figure VIA). We observed the loss of endocardial marker expression and gain of  
280 mesenchymal marker expression during the progression of the transition (Online Figure VIB).  
281 The expression of genes that have been implicated in EndoMT, particularly genes of the TGF $\beta$   
282 signaling pathway<sup>41</sup>, were positively correlated with the trajectory (Online Figure VIC).  
283 Furthermore, we identified the critical transcriptional regulators potentially involved in the  
284 transition (Online Figure VID). Interestingly, *Klf2*, encoding a TF that may play a role in EMT  
285 during cardiac development<sup>42</sup>, was found to be ranked at the top of critical regulators. The  
286 predicted targets of *Klf2* were mainly enriched for epithelial to mesenchymal transition (Online  
287 Figure VIE), and included 16 genes that have been implicated in EMT (Gene Ontology term:  
288 epithelial to mesenchymal transition; Online Figure VIF).

289 ***Convergent development of the VSMCs at the base of the great arteries is confirmed***  
290 ***by single-molecule fluorescent *in situ* hybridization***

291 To experimentally confirm myocardial to VSMC trans-differentiation, we performed single-  
292 molecule fluorescent *in situ* hybridization (smFISH) with probes for *Myh7* (myocardial marker),  
293 *Cxcl12* (VSMC marker) and *Bmp4* (the myocardial subpopulation c9 marker), which were  
294 selected based on our single-cell dataset (Figure 2D). Serial sections of the OFT at the middle

295 stage ps49 from proximal to distal clearly showed myocardial to arterial phenotypic change in  
296 OFT walls (Figure 6A). Cells expressing high levels of *Myh7* (green) in OFT walls gradually  
297 changed into cells expressing *Cxcl12* (blue) over development. Remarkably, this change  
298 occurred faster on the aortic side than on the pulmonary arterial side. In addition to OFT walls,  
299 the expression of *Cxcl12* was specifically observed in a strip of cushion mesenchymal cells  
300 between the lumens of aorta and pulmonary artery, which developed into the aorticopulmonary  
301 septum, a smooth muscle structure that eventually forms the facing walls of the great arteries.  
302 These results illustrated that *Cxcl12* could serve as an early specific marker for the VSMC  
303 lineage of the OFT. In a single section, we could observe cells expressing myocardial marker  
304 *Myh7* co-expressed various levels of *Bmp4* and the VSMC marker gene *Cxcl12*, indicating a  
305 continuum of cell state transitions during myocardial to VSMC trans-differentiation (Figure  
306 6B). The *Myh7*<sup>+</sup>*Cxcl12*<sup>low</sup>*Bmp4*<sup>high</sup> cells that we observed (right panel of Figure 6B) may  
307 correspond to the c9 myocardial subpopulation.

308 Next, we tried to validate the existence of the c8 *Penk*<sup>+</sup> mesenchymal subpopulation and confirm  
309 its role in mesenchymal to VSMC transition. Interestingly, serial sections of the OFT from  
310 proximal to distal showed that the expression of *Penk* could be observed only at the cushion  
311 mesenchyme where the fusion was occurring (the section S12, Figure 6C). We observed *Penk*<sup>+</sup>  
312 mesenchymal cells co-expressed the VSMC marker *Cxcl12*<sup>+</sup> and *Bmp4*<sup>+</sup> (left panel of Figure  
313 6D). These results suggest that the c8 *Penk*<sup>+</sup> mesenchymal subpopulation is undergoing  
314 transition to VSMCs and may be associated with the fusion of the OFT cushions. Additionally,  
315 at section S12, the co-expression of *Bmp4* and *Cxcl12* could be observed at both the  
316 mesenchyme of the aorticopulmonary septum (left panel of Figure 6D) and the myocardial free  
317 wall of the aortic side (right panel of Figure 6D), which imply that independent of the  
318 developmental paths, *Bmp4* signaling may be associated with VSMC development.

319 ***Web-based interfaces for further exploration of the single-cell data for the developing***  
320 ***OFT***

321 Our dataset constitutes a valuable resource for the scientific community to prioritize the  
322 candidate genes of OFT malformations based on expression and map the candidate genes to  
323 cell types/subpopulations. To facilitate further data exploration, we developed web-based  
324 interfaces for our dataset (<http://singlecelloft.fwgenetics.org>). These tools permit interactive  
325 examination of expression for any gene of interest, dynamic changes in cell states for each  
326 cluster in a 3D space, and potential intercellular communications among cell lineages for any  
327 ligand-receptor pair. Based on the expression of known ligand-receptor pairs, we observed  
328 extensive networks of potential intercellular communications among all cell lineages at each  
329 developmental stage (Online Figure VII). Interestingly, the network became significantly  
330 denser at the middle stage ps49 than at the other two stages, indicating increased intercellular  
331 communications at the middle stage.

## 332 DISCUSSION

333 In the present study, we performed single-cell transcriptomic sequencing of 55,611 mouse OFT  
334 cells from three successive developmental stages that generally correspond to the early, middle  
335 and late stages of OFT remodeling and septation (47, 49 and 51 pairs of somites). The large-  
336 scale single-cell data empowered us to unbiasedly and systematically dissect the cellular  
337 diversity and heterogeneity during OFT development. We identified 17 cell clusters that could  
338 be assigned to six cell lineages. Among these lineages, the macrophage and VSMC lineages of  
339 the developing OFT have seldom been previously described in detail. In accordance with the  
340 myocardial to arterial phenotypic change, we observed the myocardial lineage diminished over  
341 time, while the VSMC lineage expanded during development. We provided molecular  
342 signatures for the cell lineages and clusters, and highlighted that *Cxcl12* could serve as a specific  
343 early marker for the embryonic VSMC lineage at the base of the great arteries. Cell lineage  
344 relationships and cellular transitions, such as EndoMT, have been identified through analyzing  
345 the dynamic changes in cell states by a force-directed layout of the KNN graph. In particular,  
346 we identified convergent development of the VSMCs at the base of the great arteries that has  
347 not been recognized before, where intermediate cell subpopulations were found to be involved  
348 in either myocardial to VSMC trans-differentiation or mesenchymal to VSMC transition.  
349 Through smFISH, we observed that cells expressing the myocardial marker *Myh7* co-expressed  
350 various levels of *Bmp4* (the marker gene for the myocardial c9 cluster) and the VSMC marker  
351 gene *Cxcl12* in OFT walls, thus confirming the existence of myocardial to VSMC trans-  
352 differentiation. Moreover, we found that the *Penk<sup>+</sup>* cluster c8, a relatively small mesenchymal  
353 subpopulation that was undergoing mesenchymal to VSMC transition, was specifically  
354 associated with the fusion of the OFT cushions. Through pseudo-temporal ordering and GRN  
355 analysis, we uncovered the expression dynamics and critical transcriptional regulators  
356 potentially governing cell state transitions during OFT development. Finally, we developed  
357 web-based interactive interfaces for our dataset to facilitate further data exploration.

### 358 *Cellular diversity of developing cardiac OFT uncovered by large-scale single-cell* 359 *profiling*

360 Defining the lineage, proportion and molecular signature of distinct cell types is fundamental  
361 to our understanding of developmental processes<sup>43</sup>. Single-cell RNA-seq has revolutionized  
362 developmental biology by allowing for unbiased and systematic characterization of the cellular  
363 states in developing systems, such as the developing human fetal kidney<sup>44</sup> and prefrontal  
364 cortex<sup>45</sup>. In a study on single-cell anatomical mapping of the embryonic heart<sup>19</sup>, the authors  
365 investigated the cellular composition and gene signatures of the OFT. However, only a total of  
366 371 OFT cells (E10.5) were analyzed, which may be insufficient for a detailed dissection of  
367 heterogeneity. Apart from the four cell lineages (myocardial, epicardial, endocardial and  
368 mesenchymal) previously described<sup>19</sup>, our large-scale single-cell RNA-seq empowered us to  
369 detect a relatively rare (0.5%) cell lineage, i.e., macrophages (Figure 2B). Notably, the relative

370 proportion of macrophages did not significantly change during development (Figure 2C),  
371 implying their important role in OFT development. Given that apoptosis is a ubiquitous process  
372 during development including OFT development<sup>46</sup>, macrophages are thought to function to  
373 remove debris arising from normal apoptosis. Nevertheless, it has been increasingly recognized  
374 that macrophages residing in tissues play essential roles in normal development. For example,  
375 macrophages are required for coronary development via mediating the remodeling of the  
376 primitive coronary plexus<sup>47</sup>. Our findings highlight the role of macrophages in OFT remodeling  
377 and suggest avenues for further investigation into the role of macrophages in cardiac  
378 development.

379 We also characterized the VSMC lineage of the developing OFT which has not been described  
380 in previous studies<sup>19</sup>. Our data showed that the VSMC lineage constituted the second largest  
381 (22.3%) cell population of the developing OFT (Figure 2B) and significantly expanded over  
382 development (Figure 2C). This observation is in line with our knowledge that OFT walls  
383 undergo myocardial to arterial phenotype change during development<sup>13</sup>. Although *Cxcl12* was  
384 previously found highly expressed in the walls of the aorta and pulmonary trunk of the  
385 embryonic heart (E12.5)<sup>28</sup>, our data highlights that *Cxcl12* could serve as a specific early marker  
386 for the embryonic VSMC lineage of the great arteries (Figure 2D). Through smFISH, the  
387 expression of *Cxcl12* was observed specifically in cells that would eventually form mature  
388 smooth muscle structures. For example, *Cxcl12* was highly expressed in a strip of cushion  
389 mesenchymal cells between the lumens of aorta and pulmonary artery, which would develop  
390 into the aorticopulmonary septum, a smooth muscle structure that eventually forms the facing  
391 walls of the great arteries (Figure 6A). The chemokine *Cxcl12*, which is secreted mainly in  
392 smooth muscle cells, has been suggested to be essential for coronary artery development  
393 through driving migration of cells expressing its receptor *Cxcr4*, e.g., endothelia cells<sup>28</sup>.  
394 *Cxcl12-Cxcr4* signaling has also been suggested to be required for correct patterning of  
395 pulmonary and aortic arch arteries possibly by protecting arteries from uncontrolled sprouting<sup>48</sup>.  
396 Although the mechanism underlying the arterial system development mediated by *Cxcl12-*  
397 *Cxcr4* signaling remains elusive, our result may suggest a role in septation and remodeling of  
398 the OFT.

399 ***Intra-lineage heterogeneity of developing cardiac OFT unraveled by large-scale***  
400 ***single-cell profiling***

401 Cellular heterogeneity is a general feature of biological tissues and exists even within seemingly  
402 ‘homogeneous’ cell populations<sup>16</sup>. The large-scale single-cell RNA-seq unraveled previously  
403 unrecognized cellular heterogeneity within each cell lineage of the developing OFT. Except for  
404 macrophages, all other five cell lineages displayed distinct cell clusters/subpopulations (Figure  
405 1B, Figure 2B). *Tmem255a*, previously reported to be an epicardial marker of the embryonic  
406 heart<sup>19</sup>, was found only mark one of the two subpopulations of the OFT epicardial lineage  
407 (Figure 2D, Online Figure IV). Samples derived from each developmental stage were found to

408 have cells in almost all of these clusters, and they differ only in terms of relative proportions  
409 (Figure 1C). This result illustrates that each of our samples captured a full spectrum of cellular  
410 states throughout development due to cellular asynchrony. This finding also gave us a unique  
411 chance to identify the intermediate, transitioning subpopulations that have not been  
412 characterized before. For example, we identified c9 as a myocardial subpopulation undergoing  
413 myocardium to VSMC trans-differentiation (Figure 4). Additionally, the transcriptomic  
414 heterogeneity among subpopulations was predominately driven by the cellular positions along  
415 the transition, differentiation or maturation of cell lineages, as reflected by the dynamic changes  
416 in relative proportions over time for many clusters (Figure 1C, Figure 3C). For example, the  
417 VSMC cluster c3 rapidly expanded over development and represented a more mature state of  
418 the VSMC lineage than c4 did. Nevertheless, transcriptomic heterogeneity may also be  
419 influenced by other factors. For example, c8 represents a small mesenchymal subpopulation  
420 associated with the fusion of OFT cushions.

421 ***Myocardial to VSMC trans-differentiation occurred during the OFT development***

422 From the onset of development, the OFT is encased by a myocardial wall. As the progression  
423 of septation and remodeling, the myocardial wall rapidly changed into an arterial phenotype,  
424 characterized by the thick layer of smooth muscle cells in the tunica media. This myocardial to  
425 arterial phenotypic change has been previously described<sup>13, 49</sup>, and our smFISH with probes  
426 marking the myocardial (*Myh7*) and VSMC (*Cxcl12*) lineages on serial sections of the OFT  
427 clearly displayed this process (Figure 6A). However, the fate of the myocardium during this  
428 process remains controversial to date. It has been suggested that trans-differentiation of  
429 myocardial cells to arterial components may occur during OFT development in the embryonic  
430 hearts of chicken<sup>50</sup>, rat<sup>49</sup> and mouse<sup>51</sup>. Conversely, it is also held that the phenotypic change  
431 could just be considered a regression of the myocardium<sup>13</sup>. Our single-cell dataset supports the  
432 view of myocardial to VSMC trans-differentiation by identifying cell clusters representing a  
433 continuum of cell state transitions (Figure 3D). Expression profile comparison analysis  
434 demonstrated that myocardial cluster c9 and VSMC cluster c4 were in an intermediate state  
435 along the trajectory of myocardium to VSMC trans-differentiation (Figure 4). Through smFISH  
436 we observed that cells expressing myocardial marker *Myh7* co-expressed various levels of  
437 *Bmp4* (c9 marker gene) and VSMC marker gene *Cxcl12* in OFT walls, thus confirming the  
438 myocardial to VSMC trans-differentiation (Figure 6). A recent study demonstrated that  
439 myocardial cells may transit to the mesenchymal cells of the intercalated cushions during OFT  
440 development<sup>52</sup>. Thus, our findings provide additional evidence that highlights the plasticity of  
441 the embryonic myocardial cells of the OFT. All these findings imply that transitions between  
442 cell lineages during OFT development may be more complicated than previously appreciated.

443 ***Convergent development of the VSMCs at the base of the great arteries***

444 Cell lineage relationships and cellular state transitions can be inferred from time-series single-

445 cell transcriptomic data even for a complex developmental system, such as embryogenesis of  
446 frog<sup>53</sup> and zebrafish<sup>54</sup>, through a force-directed layout of the KNN graph. Based on the dynamic  
447 change in cell states over time reflected by the KNN graph of our time-series single-cell data,  
448 known cell transition events were recapitulated, for example, EndoMT that underwent between  
449 the endocardial and mesenchymal subpopulations (Online Figure VIA). In particular, we  
450 identified convergent development of the VSMCs at the base of the great arteries that has not  
451 been recognized before, where intermediate cell subpopulations were found to be involved in  
452 either myocardial to VSMC trans-differentiation or mesenchymal to VSMC transition (Figure  
453 3F &3G). We found that the mesenchymal to VSMC transition involved one mesenchymal  
454 subpopulation, c1, that occurred mainly at the late stage, and another smaller mesenchymal  
455 subpopulation, c8, that occurred mainly at the early stage. Such a temporal relationship for  
456 mesenchymal to VSMC transition has never been recognized before. Furthermore, by smFISH,  
457 the c8 *Penk*<sup>+</sup> subpopulation was found to be specifically associated with the fusion of OFT  
458 cushions, in line with its relatively small size and populating the early stage samples (Figure  
459 6C). In addition to the mesenchymal subpopulations, the myocardial subpopulation c9 also  
460 contributed to the development of the VSMC lineage. Altogether, three developmental paths  
461 were identified to be implicated in convergent development of VSMC lineage at the base of the  
462 great arteries, which involves different cell lineages and different subpopulations of the same  
463 lineage.

464 Furthermore, by pseudo-temporal ordering and GRN analysis, we uncovered gene expression  
465 dynamics and critical transcriptional regulators potentially governing the cell state transitions  
466 during the development of VSMCs (Figure 5, Online Figure V). The Notch signaling pathway  
467 has been known to positively regulate the specification, differentiation, and maturation of  
468 VSMCs<sup>38</sup>. We found that the expression of genes in the Notch signaling pathway, including  
469 receptor (*Notch1*), ligand (*Jag1*) and downstream targets (*Hey1*, *Hey2*, *Heyl* and *Pdgfrb*), was  
470 positively correlated with the reconstructed trajectories for all the three paths. Then, we  
471 identified *Heyl*, encoding a known downstream TF of the Notch signaling, at the top of the up-  
472 regulated regulators. Thus, our results highlight the role of the Notch signaling pathway in the  
473 development of the OFT VSMC lineage. We provide a set of critical transcriptional regulators  
474 that were sequentially activated or repressed along the development trajectory. For many of  
475 these regulators, the roles in VSMC development have seldom been suggested before.

476 In conclusion, through large-scale single-cell transcriptomic sequencing, we performed an  
477 unbiased and systematic study on the cellular types and states of the cardiac OFT during  
478 development. Our results support the existence of myocardial to VSMC trans-differentiation,  
479 and convergent development of the VSMC lineage at the base of the great arteries. We provide  
480 a single-cell reference map of cell states for normal OFT development, which allows the CHD  
481 community to assess how perturbations affect the transcriptomic states of OFT cell lineages, to  
482 prioritize candidate genes of OFT malformations based on expression, and to map candidate  
483 genes to cell types or subpopulations. Our study demonstrated the power of time-series single-  
484 cell transcriptomic data for identifying cell state transitions in a complex developmental system.

485 **ACKNOWLEDGMENTS**

486 We thank the staff in the public platform of the State Key Laboratory of Cardiovascular Disease  
487 for providing technical assistance.

488 **SOURCES OF FUNDING**

489 This work is supported by grants from the CAMS Initiative for Innovative Medicine (2016-  
490 I2M-1-016) and the Post-doctoral International Exchange Project of Peking Union Medical  
491 College.

492 **DISCLOSURES**

493 None

494 **REFERENCES**

- 495 1. van der Linde D, Konings EE, Slager MA, Witsenburg M, Helbing WA, Takkenberg JJ and Roos-  
496 Hesselink JW. Birth prevalence of congenital heart disease worldwide: a systematic review and meta-  
497 analysis. *J Am Coll Cardiol.* 2011;58:2241-2247.
- 498 2. Thom T, Haase N, Rosamond W, Howard VJ, Rumsfeld J, Manolio T, Zheng Z-J, Flegal K,  
499 O'donnell C and Kittner S. Heart disease and stroke statistics—2006 update: a report from the American  
500 Heart Association Statistics Committee and Stroke Statistics Subcommittee. *Circulation.* 2006;113:e85-  
501 e151.
- 502 3. Neeb Z, Lajiness JD, Bolanis E and Conway SJ. Cardiac outflow tract anomalies. *Wiley Interdiscip*  
503 *Rev Dev Biol.* 2013;2:499-530.
- 504 4. Kelly RG, Buckingham ME and Moorman AF. Heart fields and cardiac morphogenesis. *Cold Spring*  
505 *Harb Perspect Med.* 2014;4.
- 506 5. Eriksson G, Liestøl K, Seem E, Birkeland S, Saatvedt KJ, Hoel TN, Døhlen G, Skulstad H,  
507 Svennevig JL and Thaulow E. Achievements in congenital heart defect surgery: a prospective, 40-year  
508 study of 7038 patients. *Circulation.* 2015;131:337-346.
- 509 6. Webb S, Qayyum SR, Anderson RH, Lamers WH and K Richardson M. Septation and separation  
510 within the outflow tract of the developing heart. *J Anat.* 2003;202:327-342.
- 511 7. Verzi MP, McCulley DJ, De Val S, Dodou E and Black BL. The right ventricle, outflow tract, and  
512 ventricular septum comprise a restricted expression domain within the secondary/anterior heart field.  
513 *Dev Biol.* 2005;287:134-145.
- 514 8. Eisenberg LM and Markwald RR. Molecular regulation of atrioventricular valvuloseptal  
515 morphogenesis. *Circ Res.* 1995;77:1-6.
- 516 9. Plein A, Fantin A and Ruhrberg C. Neural crest cells in cardiovascular development. *Curr Top Dev*  
517 *Biol.* 2015;111:183-200.
- 518 10. Lin CJ, Lin CY, Chen CH, Zhou B and Chang CP. Partitioning the heart: mechanisms of cardiac  
519 septation and valve development. *Development.* 2012;139:3277-3299.
- 520 11. Kelly RG and Buckingham ME. The anterior heart-forming field: voyage to the arterial pole of the

521 heart. *Trends Genet.* 2002;18:210-216.

522 12. von Gise A and Pu WT. Endocardial and epicardial epithelial to mesenchymal transitions in heart  
523 development and disease. *Circ Res.* 2012;110:1628-45.

524 13. Anderson RH, Webb S, Brown NA, Lamers W and Moorman A. Development of the heart: (3)  
525 formation of the ventricular outflow tracts, arterial valves, and intrapericardial arterial trunks. *Heart.*  
526 2003;89:1110-8.

527 14. Zheng GX, Terry JM, Belgrader P, Ryvkin P, Bent ZW, Wilson R, Ziraldo SB, Wheeler TD,  
528 McDermott GP, Zhu J, Gregory MT, Shuga J, Montesclaros L, Underwood JG, Masquelier DA,  
529 Nishimura SY, Schnall-Levin M, Wyatt PW, Hindson CM, Bharadwaj R, Wong A, Ness KD, Beppu LW,  
530 Deeg HJ, McFarland C, Loeb KR, Valente WJ, Ericson NG, Stevens EA, Radich JP, Mikkelsen TS,  
531 Hindson BJ and Bielas JH. Massively parallel digital transcriptional profiling of single cells. *Nat  
532 Commun.* 2017;8:14049.

533 15. Potter SS. Single-cell RNA sequencing for the study of development, physiology and disease. *Nat  
534 Rev Nephrol.* 2018;14:479-492.

535 16. Wen L and Tang F. Single-cell sequencing in stem cell biology. *Genome Biol.* 2016;17:71.

536 17. Herring CA, Chen B, McKinley ET and Lau KS. Single-Cell Computational Strategies for Lineage  
537 Reconstruction in Tissue Systems. *Cell Mol Gastroenterol Hepatol.* 2018;5:539-548.

538 18. DeLaughter DM, Bick AG, Wakimoto H, McKean D, Gorham JM, Kathiriya IS, Hinson JT, Homsy  
539 J, Gray J, Pu W, Bruneau BG, Seidman JG and Seidman CE. Single-Cell Resolution of Temporal Gene  
540 Expression during Heart Development. *Dev Cell.* 2016;39:480-490.

541 19. Li G, Xu A, Sim S, Priest JR, Tian X, Khan T, Quertermous T, Zhou B, Tsao PS, Quake SR and Wu  
542 SM. Transcriptomic Profiling Maps Anatomically Patterned Subpopulations among Single Embryonic  
543 Cardiac Cells. *Dev Cell.* 2016;39:491-507.

544 20. Pinto AR, Ilinykh A, Ivey MJ, Kuwabara JT, D'Antoni ML, Debuque R, Chandran A, Wang L, Arora  
545 K, Rosenthal NA and Tallquist MD. Revisiting Cardiac Cellular Composition. *Circ Res.* 2016;118:400-  
546 9.

547 21. Skelly DA, Squiers GT, McLellan MA, Bolisetty MT, Robson P, Rosenthal NA and Pinto AR.  
548 Single-cell transcriptional profiling reveals cellular diversity and intercommunication in the mouse Heart.  
549 *Cell Rep.* 2018;22:600-610.

550 22. Gautier EL, Shay T, Miller J, Greter M, Jakubzick C, Ivanov S, Helft J, Chow A, Elpek KG,  
551 Gordonov S, Mazloom AR, Ma'ayan A, Chua WJ, Hansen TH, Turley SJ, Merad M, Randolph GJ and  
552 Immunological Genome C. Gene-expression profiles and transcriptional regulatory pathways that  
553 underlie the identity and diversity of mouse tissue macrophages. *Nat Immunol.* 2012;13:1118-28.

554 23. Rudat C, Grieskamp T, Röhr C, Airik R, Wrede C, Hegermann J, Herrmann BG, Schuster-Gossler  
555 K and Kispert A. Upk3b is dispensable for development and integrity of urothelium and mesothelium.  
556 *PLOS ONE.* 2014;9:e112112.

557 24. Narumiya H, Hidaka K, Shirai M, Terami H, Aburatani H and Morisaki T. Endocardiogenesis in  
558 embryoid bodies: novel markers identified by gene expression profiling. *Biochem Biophys Res Commun.*  
559 2007;357:896-902.

560 25. Wilczewski CM, Hepperla AJ, Shimbo T, Wasson L, Robbe ZL, Davis IJ, Wade PA and Conlon FL.  
561 CHD4 and the NuRD complex directly control cardiac sarcomere formation. *Proc Natl Acad Sci U S A.*  
562 2018;115:6727-6732.

563 26. Gunaje JJ, Bahrami AJ, Schwartz SM, Daum G and Mahoney Jr WM. PDGF-dependent regulation

564 of regulator of G protein signaling-5 expression and vascular smooth muscle cell functionality. *Am J*  
565 *Physiol Cell Physiol*. 2011;301:C478-C489.

566 27. Daniel J-M, Prock A, Dutzmann J, Sonnenschein K, Thum T, Bauersachs J and Sedding DG.  
567 Regulator of G-protein signaling 5 prevents smooth muscle cell proliferation and attenuates neointima  
568 formation. *Arterioscler Thromb Vasc Biol*. 2016;36:317-327.

569 28. Ivins S, Chappell J, Vernay B, Suntharalingham J, Martineau A, Mohun TJ and Scambler PJ. The  
570 CXCL12/CXCR4 axis plays a critical role in coronary artery development. *Dev Cell*. 2015;33:455-468.

571 29. Sinha S, Iyer D and Granata A. Embryonic origins of human vascular smooth muscle cells:  
572 implications for in vitro modeling and clinical application. *Cell Mol Life Sci*. 2014;71:2271-88.

573 30. Rudat C and Kispert A. Wt1 and epicardial fate mapping. *Circ Res*. 2012;111:165-169.

574 31. Henderson DJ and Copp AJ. Versican expression is associated with chamber specification, septation,  
575 and valvulogenesis in the developing mouse heart. *Circ Res*. 1998;83:523-532.

576 32. Mahdavi V, Periasamy M and Nadal-Ginard B. Molecular characterization of two myosin heavy  
577 chain genes expressed in the adult heart. *Nature*. 1982;297:659.

578 33. Xu K, Chong DC, Rankin SA, Zorn AM and Cleaver O. Rasip1 is required for endothelial cell  
579 motility, angiogenesis and vessel formation. *Dev Biol*. 2009;329:269-279.

580 34. Spencer JA, Hacker SL, Davis EC, Mecham RP, Knutsen RH, Li DY, Gerard RD, Richardson JA,  
581 Olson EN and Yanagisawa H. Altered vascular remodeling in fibulin-5-deficient mice reveals a role of  
582 fibulin-5 in smooth muscle cell proliferation and migration. *Proc Natl Acad Sci U S A*. 2005;102:2946-  
583 2951.

584 35. Weinreb C, Wolock S, Klein AM and Berger B. SPRING: a kinetic interface for visualizing high  
585 dimensional single-cell expression data. *Bioinformatics*. 2018;34:1246-1248.

586 36. Xu J and Shi G-P. Vascular wall extracellular matrix proteins and vascular diseases. *Biochim*  
587 *Biophys Acta Mol Basis Dis*. 2014;1842:2106-2119.

588 37. Pandya K and Smithies O.  $\beta$ -MyHC and cardiac hypertrophy: size does matter. *Circ Res*.  
589 2011;109:609-610.

590 38. Fouillade C, Monet-Lepretre M, Baron-Menguy C and Joutel A. Notch signalling in smooth muscle  
591 cells during development and disease. *Cardiovasc Res*. 2012;95:138-46.

592 39. Singh R and Kispert A. Tbx20, Smads, and the atrioventricular canal. *Trends Cardiovasc Med*.  
593 2010;20:109-114.

594 40. Lin Q, Lu J, Yanagisawa H, Webb R, Lyons GE, Richardson JA and Olson EN. Requirement of the  
595 MADS-box transcription factor MEF2C for vascular development. *Development*. 1998;125:4565-4574.

596 41. Cho JG, Lee A, Chang W, Lee M-S and Kim J. Endothelial to mesenchymal transition represents a  
597 key link in the interaction between inflammation and endothelial dysfunction. *Front Immunol*. 2018;9.

598 42. Chiplunkar AR, Lung TK, Alhashem Y, Koppenhaver BA, Salloum FN, Kukreja RC, Haar JL and  
599 Lloyd JA. Krüppel-like factor 2 is required for normal mouse cardiac development. *PLOS ONE*.  
600 2013;8:e54891.

601 43. Griffiths JA, Scialdone A and Marioni JC. Using single-cell genomics to understand developmental  
602 processes and cell fate decisions. *Mol Syst Biol*. 2018;14:e8046.

603 44. Wang P, Chen Y, Yong J, Cui Y, Wang R, Wen L, Qiao J and Tang F. Dissecting the global dynamic  
604 molecular profiles of human fetal kidney development by single-cell RNA sequencing. *Cell Rep*.  
605 2018;24:3554-3567.e3.

606 45. Zhong S, Zhang S, Fan X, Wu Q, Yan L, Dong J, Zhang H, Li L, Sun L, Pan N, Xu X, Tang F,

607 Zhang J, Qiao J and Wang X. A single-cell RNA-seq survey of the developmental landscape of the human  
608 prefrontal cortex. *Nature*. 2018;555:524-528.

609 46. Fisher SA, Langille BL and Srivastava D. Apoptosis during cardiovascular development. *Circ Res*.  
610 2000;87:856-864.

611 47. Leid J, Carrelha J, Boukarabila H, Epelman S, Jacobsen SEW and Lavine KJ. Primitive embryonic  
612 macrophages are required for coronary development and maturation. *Circ Res*. 2016;118:1498-1511.

613 48. Kim BG, Kim YH, Stanley EL, Garrido-Martin EM, Lee YJ and Oh SP. CXCL12-CXCR4  
614 signalling plays an essential role in proper patterning of aortic arch and pulmonary arteries. *Cardiovasc  
615 Res*. 2017;113:1677-1687.

616 49. Ya J, van den Hoff MJ, de Boer PA, Tesink-Taekema S, Franco D, Moorman AF and Lamers WH.  
617 Normal development of the outflow tract in the rat. *Circ Res*. 1998;82:464-72.

618 50. Argüello C, Mv DLC and Sánchez C. Ultrastructural and experimental evidence of myocardial cell  
619 differentiation into connective tissue cells in embryonic chick heart. *J Mol Cell Cardiol*. 1978;10:307-  
620 315.

621 51. Yang YP, Li HR and Jing Y. Septation and shortening of outflow tract in embryonic mouse heart  
622 involve changes in cardiomyocyte phenotype and  $\alpha$ -SMA positive cells in the endocardium. *Chin Med J  
(Engl)*. 2004;117:1240-1245.

624 52. Mifflin JJ, Dupuis LE, Alcala NE, Russell LG and Kern CB. Intercalated cushion cells within the  
625 cardiac outflow tract are derived from the myocardial troponin T type 2 (Tnnt2) Cre lineage. *Dev Dyn*.  
626 2018;247:1005-1017.

627 53. Briggs JA, Weinreb C, Wagner DE, Megason S, Peshkin L, Kirschner MW and Klein AM. The  
628 dynamics of gene expression in vertebrate embryogenesis at single-cell resolution. *Science*.  
629 2018;360:eaar5780.

630 54. Wagner DE, Weinreb C, Collins ZM, Briggs JA, Megason SG and Klein AM. Single-cell mapping  
631 of gene expression landscapes and lineage in the zebrafish embryo. *Science*. 2018;360:pp. 981-987.

632

633 **FIGURE LEGENDS**

634 **Figure 1. Single-cell transcriptomic sequencing and unbiased clustering of cells during**  
635 **OFT development.** **(A)** Overview of the experimental procedure. Single-cell suspensions from  
636 three successive stages of mouse OFT development were captured and sequenced separately.  
637 Two biological replicates were prepared for each stage. ps47, ps49 and ps51 denote 47, 49 and  
638 51 pairs of somites, respectively. Dissection boundaries are indicated by the red dotted lines on  
639 the schematic plots of embryonic hearts. **(B)** Unsupervised clustering of all cells reveals 17 cell  
640 clusters projected on a two-dimensional tSNE map. **(C)** Fraction of cells derived from each  
641 sample for each cluster. All samples are normalized to the same number of cells (4,270).

642 **Figure 2. Cellular diversity and gene signatures of the developing OFT identified by**  
643 **single-cell transcriptomic analysis.** **(A)** Cell lineages recognized by known cell-type specific  
644 marker genes. Each cell is colored according to the scaled expression of the indicated marker  
645 gene. **(B)** Relatedness of clusters revealed by hierarchical clustering. This analysis is based on  
646 the average expression of the 1,381 HVGs in each cluster. **(C)** Cell fractions of each stage for  
647 each cell lineage. The average cell fraction of the two biological replicates and the standard  
648 error are shown on the bar plot. ‘ns’: not significant; \*: Student's t-Test P-value < 0.05; \*\*:  
649 Student's t-Test P-value < 0.01. In B and C, all samples are normalized to the same number of  
650 cells (4,270). **(D)** Gene signature for each cell lineage or cluster. These genes were identified  
651 and selected by differential expression analysis and random forest classification. The schematic  
652 plot represents a cross section of OFT in a specific position where the aorta wall shows an artery  
653 phenotype while the wall of the pulmonary artery still possesses a myocardial phenotype. The  
654 two small myocardial clusters c14 and c16 were not incorporated in this analysis. EP: epicardial;  
655 MS: mesenchymal; MC: myocardial; ED: endocardial; VSMC: vascular smooth muscle cell

656 **Figure 3. Convergent development of the VSMCs at the base of the great arteries.** **(A)**  
657 Force-directed layout of a KNN graph showing a continuous expression topology of the OFT  
658 cellulome during development. Each dot denotes a cell colored by cell cluster. **(B)** KNN graph  
659 colored by development stage. **(C)** Dynamic changes of cell states over time. Cells colored in  
660 gray denote those from other stages. All samples are normalized to the same number of cells  
661 (4,270). **(D)** Dynamic changes of cell clusters directly involved in VSMC development. **(E)**  
662 Relative proportions of cell clusters directly involved in VSMC development. **(F)** Inferred  
663 developmental paths of the smooth muscle cells displayed on the KNN graph. **(G)** Inferred  
664 developmental paths of the smooth muscle cells displayed on the tSNE plot.

665 **Figure 4. Characteristics of gene expression profiles for the intermediate cell**  
666 **subpopulations during myocardial to VSMC trans-differentiation.** **(A)** Heatmap showing  
667 the DEGs between myocardial cluster c2 and c9. **(B)** Significant expression differences of some  
668 key marker genes between c2 and c9. Each dot denotes a cell. **(C)** The ratio of *Myh6* to *Myh7*  
669 in c2 and c9. **(D)** Functional enrichment of genes significantly up-regulated in c9. **(E)** Heatmap  
670 showing the DEGs between the VSMC cluster c3 and the intermediate VSMC population c4.  
671 **(F)** Significant expression differences of some key marker genes between c3 and c4. **(G)**  
672 Functional enrichment of genes significantly up-regulated in c3.

673 **Figure 5. Pseudo-temporal ordering and GRN analysis uncover critical transcriptional**  
674 **regulators potentially governing cell state transitions during the development of VSMCs.**  
675 **(A)** Loss of myocardial marker expression and gain of VSMC marker expression during  
676 myocardial to VSMC trans-differentiation. **(B)** Expression of genes in the Notch signaling is  
677 positively correlated with the trajectory of myocardial to VSMC trans-differentiation. **(C)**  
678 Critical transcriptional regulators potentially involved in myocardial to VSMC trans-  
679 differentiaton. **(D)** Loss of mesenchymal marker expression and gain of VSMC marker  
680 expression during c8 mesenchymal to VSMC transition. **(E)** Expression of genes in the Notch  
681 signaling is positively correlated with the trajectory of c8 mesenchymal to VSMC transition.  
682 **(F)** Critical transcriptional regulators potentially involved in c8 mesenchymal to VSMC  
683 transition. ●: VSMC marker; ▲: myocardial marker; ★: mesenchymal marker.

684 **Figure 6. Convergent development of the VSMCs at the base of the great arteries is**  
685 **confirmed by smFISH.** **(A)** Serial sections of the OFT at stage ps49 from proximal to distal  
686 showing myocardial to arterial phenotypic change in the OFT walls. Green: *Myh7*; Blue: *Cxcl12*;  
687 Red: *Bmp4*. Scale bar: 50  $\mu$ m. The aorta is arranged on the upper side. **(B)** Myocardial to VSMC  
688 trans-differentiation is supported by the observation that cells expressing myocardial marker  
689 *Myh7* co-express various levels of *Bmp4* and VSMC marker gene *Cxcl12*. Middle panel: section  
690 S18; The yellow dotted line shows the border of the lumen of aorta (A) and pulmonary trunk  
691 (P); AS: aorticopulmonary septum. Left panel: *Myh7*<sup>+</sup>*Cxcl12*<sup>high</sup>*Bmp4*<sup>low</sup> cells; Right panel:  
692 *Myh7*<sup>+</sup>*Cxcl12*<sup>low</sup>*Bmp4*<sup>high</sup> cells. **(C)** Serial sections of the OFT at the stage ps49 from proximal  
693 to distal showing that the c8 *Penk*<sup>+</sup> mesenchymal subpopulation is undergoing transition to  
694 VSMCs and is associated with the fusion of the OFT cushions. Green: *Penk*; Blue: *Cxcl12*; Red:  
695 *Bmp4*. Scale bar: 50  $\mu$ m. **(D)** Co-expression of *Penk*, *Cxcl12* and *Bmp4*. The arrow indicates  
696 the location where the fusion is occurring. Middle panel: section S12; Left panel:  
697 *Penk*<sup>+</sup>*Cxcl12*<sup>+</sup>*Bmp4*<sup>+</sup> cells; Right panel: *Penk*<sup>+</sup>*Cxcl12*<sup>low</sup>*Bmp4*<sup>high</sup> cells.

698

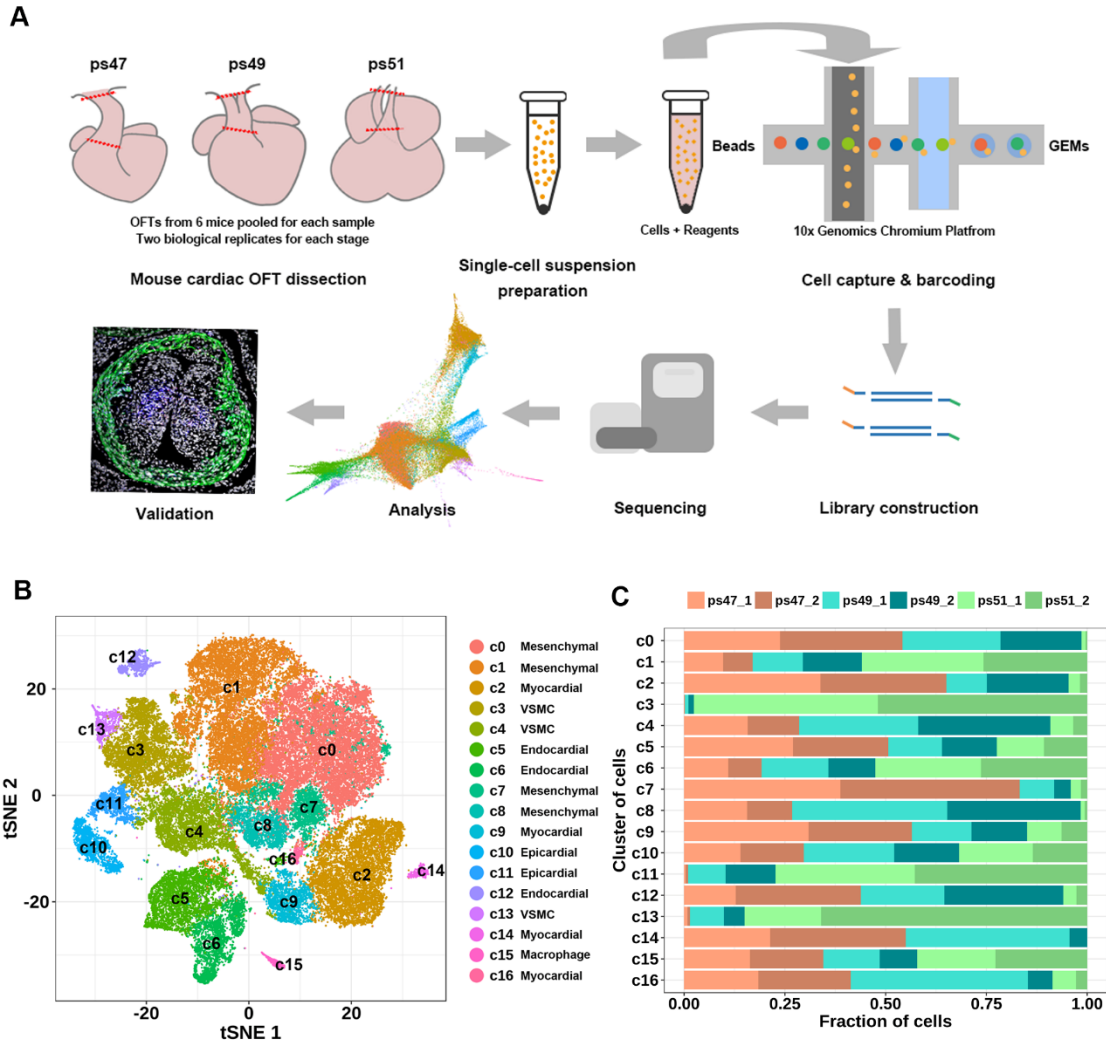


Figure 1

700

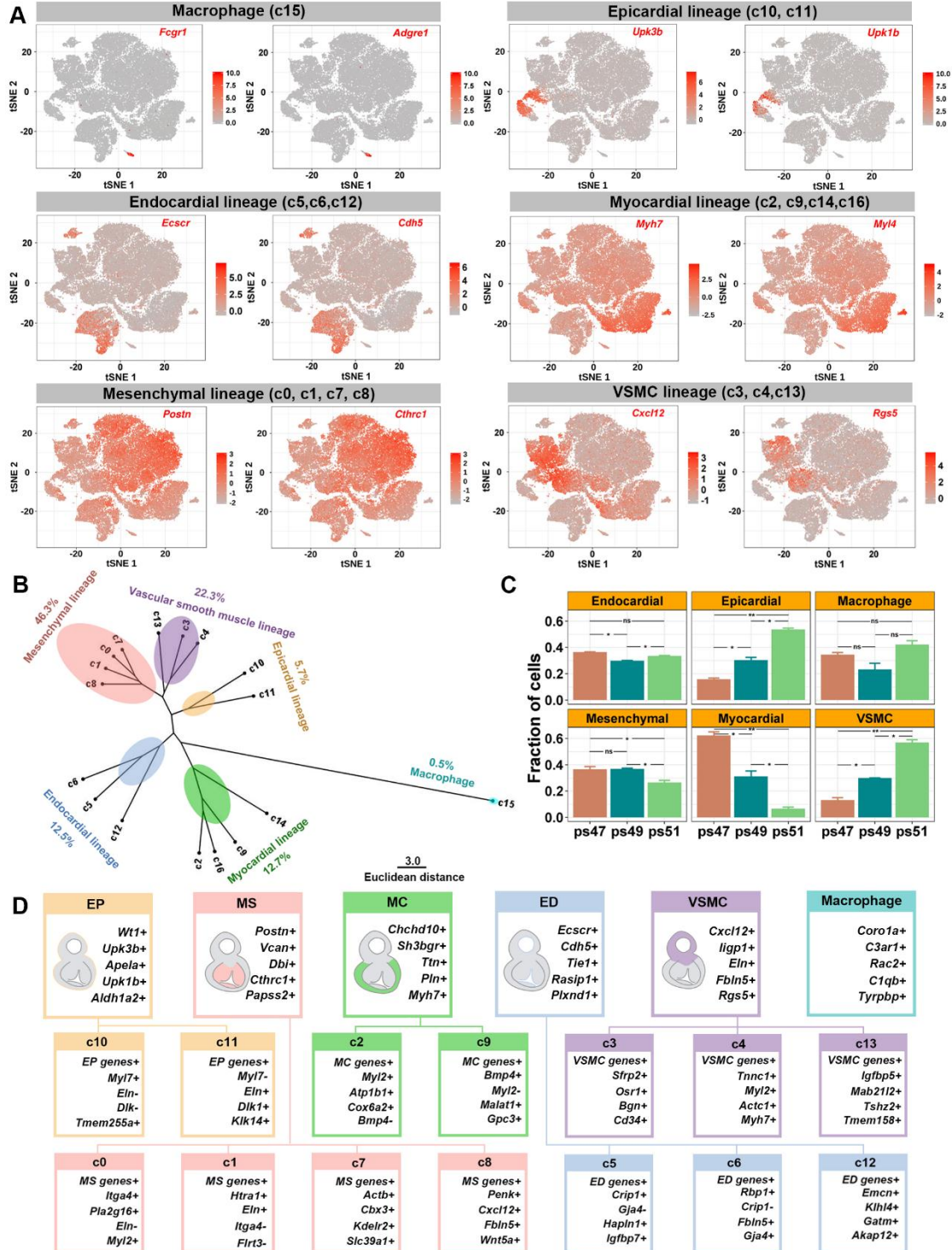
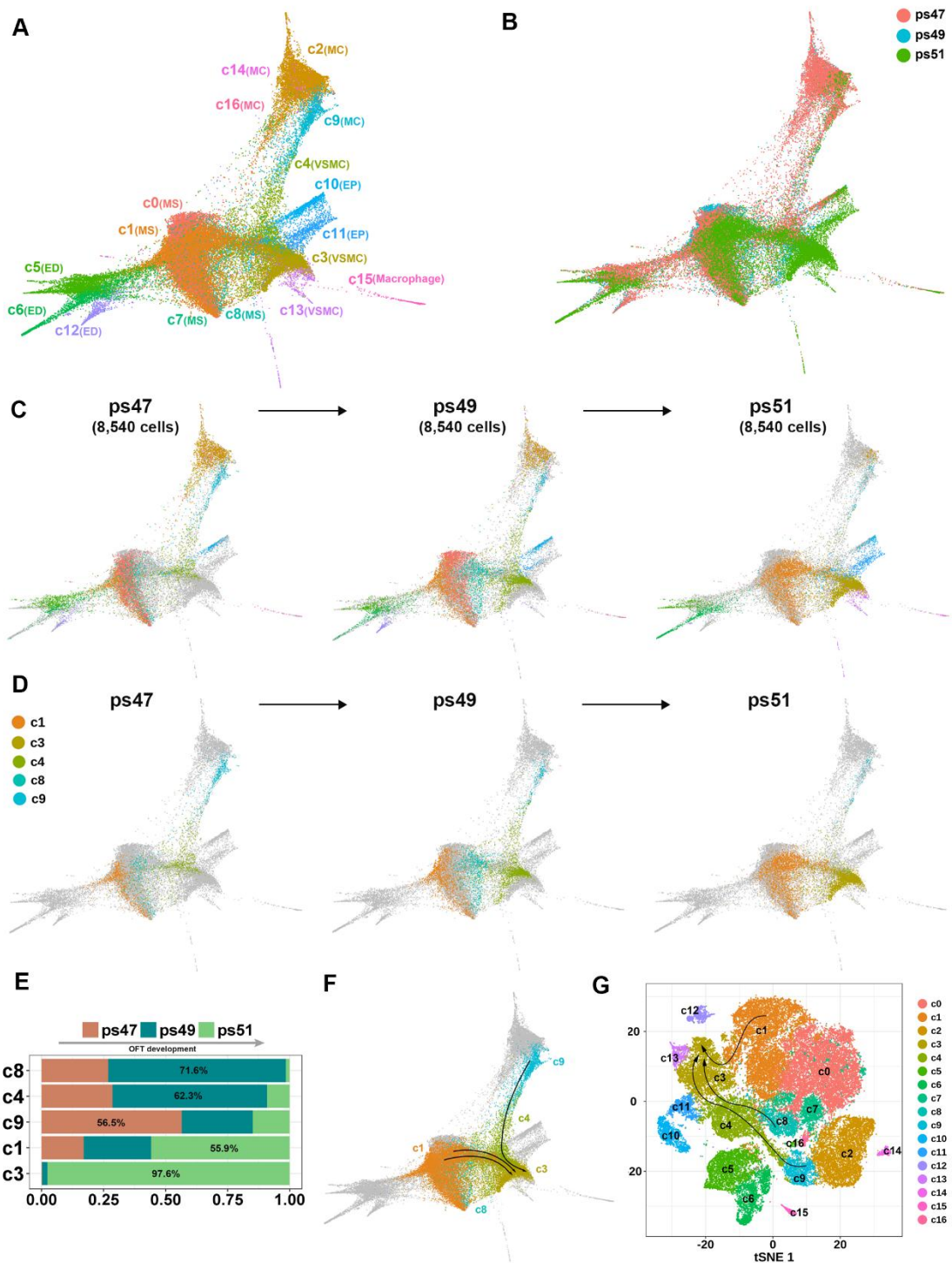


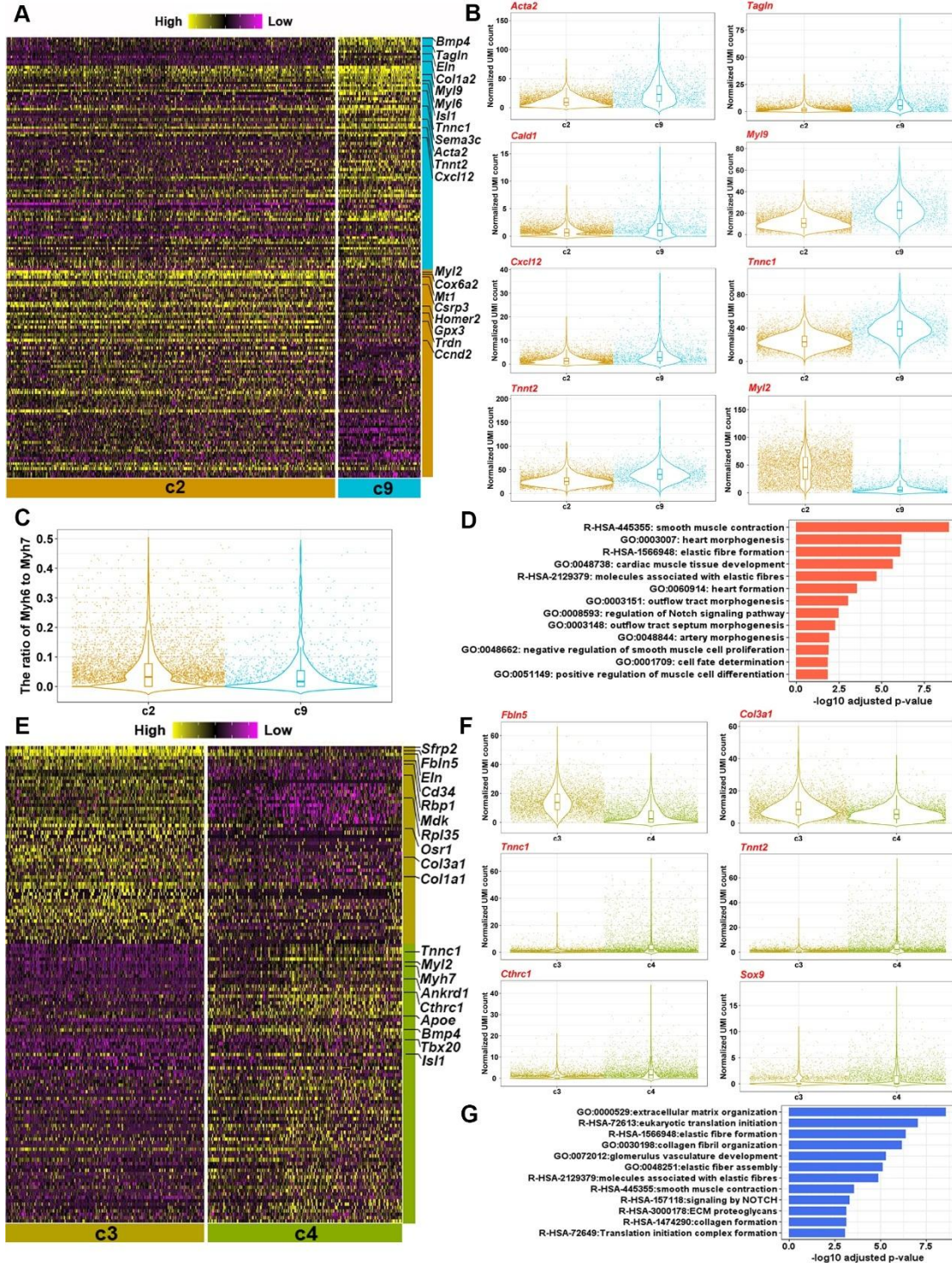
Figure 2



703

704

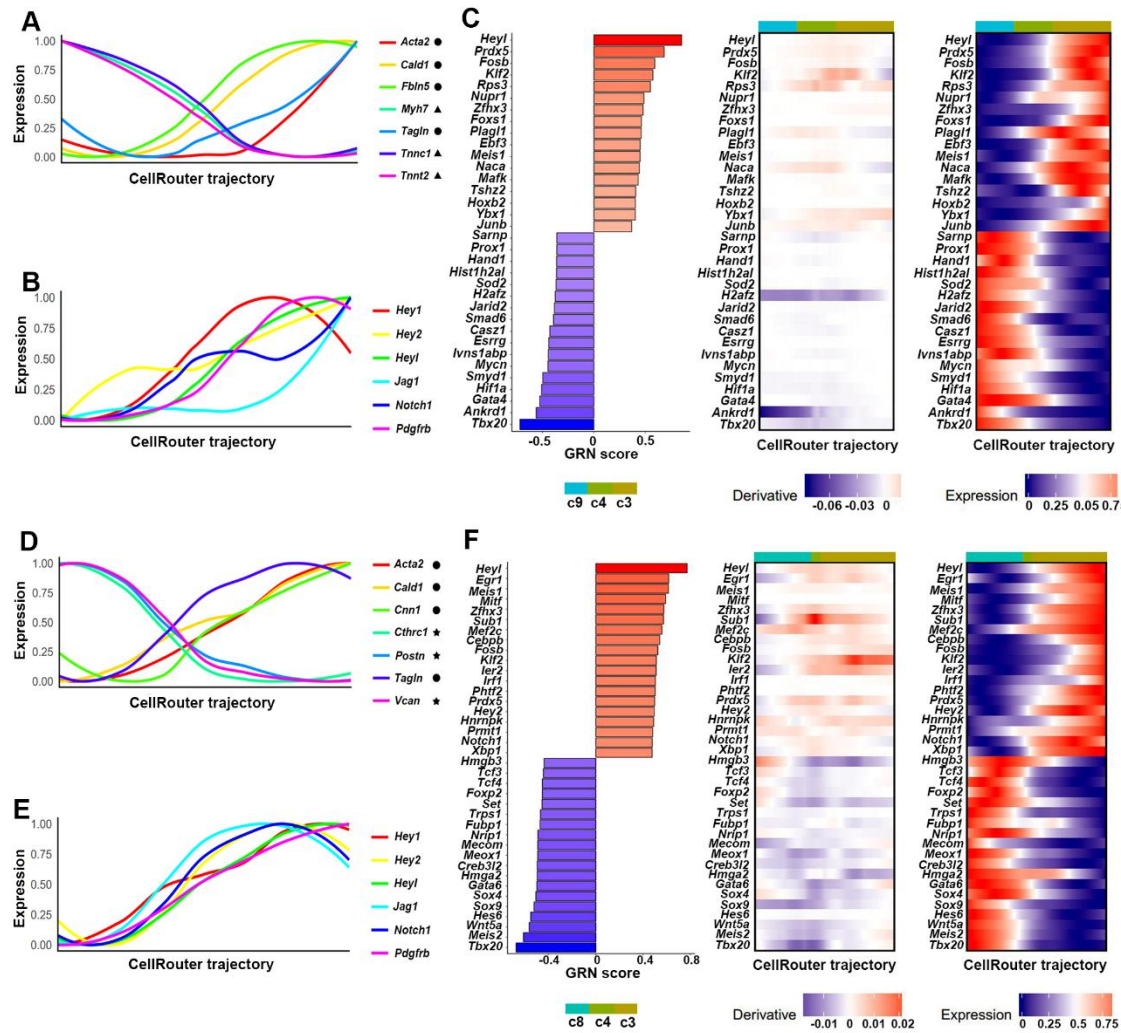
Figure 3



705

706

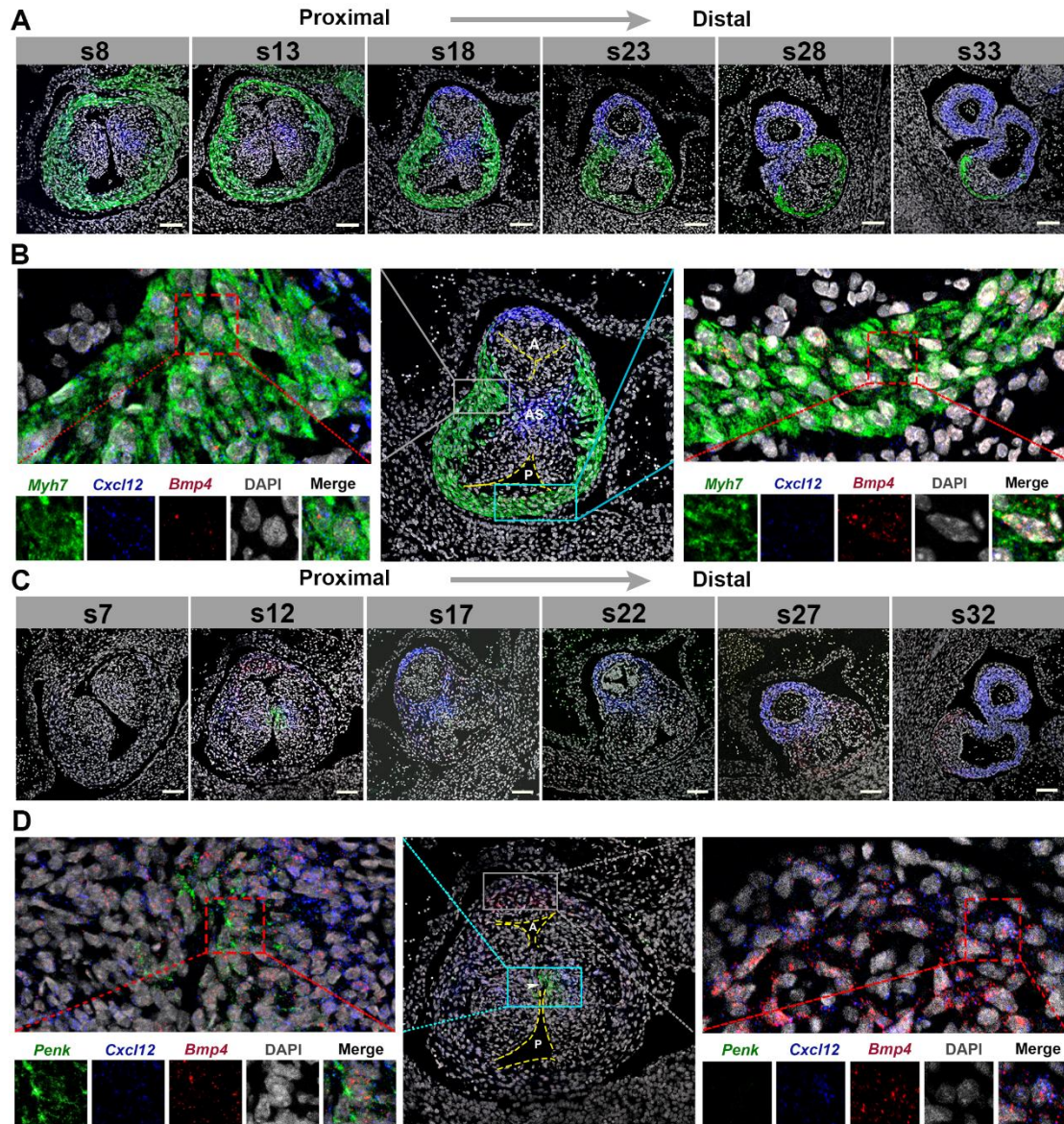
Figure 4



707

708

Figure 5



710

**Figure 6**